Atlantic Southern Ocean Productivity: Fertilization From Above or Below?

Nicholas Meskhidze[1,*], Athanasios Nenes[1,2], William L. Chameides[3], Chao Luo[4] and Natalie Mahowald[5]

[1] School of Earth and Atmospheric Sciences, Georgia Institute of Technology, Atlanta GA, 30332
[2] School of Chemical and Biomolecular Engineering, Georgia Institute of Technology, Atlanta, GA, 30332
[3] Chief Scientist, Environmental Defense, 257 Park Avenue South, New York, NY 10010
[4]Institute for Computational Earth System Science, University of California, Santa Barbara, CA, 93106
[5] National Center for Atmospheric Research, Boulder, CO, 80307

[*] Present address: Department of Marine, Earth, and Atmospheric Sciences, North Carolina State University, Raleigh, NC 27695, USA.

Primary productivity and the associated uptake of atmospheric carbon dioxide in the Southern Ocean (SO) is thought to be generally limited by bioavailable iron (Fe). Two sources of Fe for the surface waters of the SO have been proposed: (i) Oceanic input of nutrient-rich (i.e. Fe) waters from upwelling and lateral flows from continental margins; and (ii) Atmospheric input from the deposition of mineral dust emanating from the arid regions of South America and Australia. In this work, analysis of weekly remotely sensed sea surface temperature (SST), ocean chlorophyll *a* content [Chl *a*] and model-derived atmospheric dust-Fe fluxes are used to identify the predominate source of Fe during phytoplankton blooms in the surface waters of the South Atlantic Ocean between 40°–60°S. The results of our study suggest that oceanic source through upwelling of nutrient-rich waters due to mesoscale frontal dynamics is the major source of bioavailable Fe controlling biological activity in this region. This result is consistent with the idea that acidification of aeolian dust prior to it deposition to the ocean may be required to solubilize the large fraction of mineral-iron and make it bioavailable.

1. Introduction

The availability of iron (Fe) may control primary productivity in much of the world ocean, particularly in high-nitrate low-chlorophyll (HNLC) regions (Martin and Fitzwater, 1988; Coale et al., 1996; Boyd et al., 2000; Fung et al., 2000). These Fe-limited HNLC waters comprise ~30% of the world ocean (de Baar and Boyd, 2000) and thus the supply of Fe to the surface waters of the ocean may play a key role in regulating ocean productivity, the atmospheric CO_2 concentration and climate. In fact, the hypothesis that the glacial-interglacial change of atmospheric CO_2 can be attributed to changes in the atmospheric dust-Fe supply to the Southern Ocean (SO) is plausible, albeit controversial (e.g., Martin, and Fitzwater, 1988; Watson et al., 2000; Maher and Dennis, 2001; Latimer and Filippelli, 2001; Röthlisberger et al., 2004). Understanding the biogeochemical cycling of Fe in both present and past climate regimes and the role of mineral dust in Fe-mediated carbon sequestration in the oceans is one of the most outstanding issues in climate science today (Martin, and Fitzwater, 1988; Watson et al., 2000; Maher and Dennis, 2001).

The SO is one of the largest regions (e.g., Fung et al., 2000; Watson, 2001; Coale et al., 2004) of the world ocean where phytoplankton growth rates are limited by micronutrient Fe, although strong grazing pressure, light limitation and silicon limitation have also been suggested (Mitchell et al., 1991; Banse, 1996; Boyd et al., 2001; Coale et al., 2004). Due to the large silicic acid gradient in the SO surface waters Fe-enrichment would cause diatoms to bloom to the south of the Antarctic Polar Front Zone (see Supplementary Information), whereas nonsiliceous phytoplankton species would likely dominate in waters to the north (Coale et al., 2004). Therefore, surface waters in the northern subantarctic region of the SO (with low silicic acid but high nitrate) are also referred as high-nitrate low-silicic acid low- chlorophyll (HNLSiLC) (Dugdale and Wilkerson, 1998). Compared to other Fe-limited regions, the SO is thought to receive the lowest flux of atmospheric dust-Fe (Duce, and Tindale, 1991) and, as a result, oceanic sources, through the upwelling of deep water, resuspension of sediments, remineralization of sinking material and diffusion from the pore waters have often been proposed to be the likely suppliers of Fe to this region (de Baar et al., 1995; Löscher et al., 1997; Watson, 2001). However, there has been a growing interest in the possible contribution of aeolian dust-Fe to the enhancement of phytoplankton stocks and concomitant drawdown of atmospheric CO_2 in this oceanic region (Maher and Dennis, 2001; Latimer and Filippelli, 2001). Two major source areas for aeolian dust deposited to the SO are arid and semi-arid regions of South America and Australia (Fung et al., 2000; Ginoux et al., 2001; Zender et al., 2003). Analysis of remotely sensed data of aerosol optical depth and ocean surface chlorophyll concentration [Chl *a*] together with the simulated dust-Fe deposition showed a strong correlation between the atmospheric delivery of mineral dust and phytoplankton growth in surface waters of the SO downwind from the Patagonian and south Australian regions (Gabric et al., 2002; Erickson et al., 2003). Based on this correlation, it has been suggested that phytoplankton productivity in the Antarctic Circumpolar Current (ACC) region of the SO between 40° - 60°S is controlled by the rate of supply of atmospheric dust-Fe mainly emanating from Patagonia (Erickson et al., 2003).

Studies suggesting a link between mineral dust deposition and productivity in the SO are subject to some uncertainties: (i) The individual dust storm event-based analysis of mineral-Fe supply to the surface waters of the SO provided no compelling evidence for a causal relationship between Australian dust deposition and phytoplankton blooms (Boyd et al., 2004); (ii) The deposition of mineral dust to Fe-limited surface ocean regions does not necessarily initiate a phytoplankton bloom. While mostly dissolved Fe can be used by phytoplankton, virtually all Fe in soils from arid and semi-arid regions is in a crystalline Fe-III form (Claquin et al., 1999), dissolution of which is believed to be negligible in first 24 hours after dust deposition to the ocean surface and extremely low thereafter (Jickells and Spokes, 2001; Bonnet and Guieu, 2004). It has been shown that dust plumes may not always exhibit enhanced soluble Fe levels relative to non-dust days (Meskhidze et al., 2005). Since Fe-III oxides can be dissolved in acidic solutions, it has been proposed that the fraction of Fe in airborne mineral dust that is mobilized or dissolved (referred to here as the Dissolved Iron Fraction or DIF) during dust transport in the atmosphere can become significant if the dust is sufficiently acidified by the incorporation of sulfuric acid from oxidation of SO_2 (Jickells and Spokes, 2001; Colin et al., 1990; Zhu et al., 1993; Zhuang et al., 1992; Meskhidze et al., 2003). Meskhidze et al. (2005) recently suggested that the amount of SO_2 entrained from the oxidation of dimethyl sulfide (DMS) alone may not be sufficient to yield the required DIF in dust storms to cause observable changes in marine ecosystem productivity. Considerable amounts of anthropogenic SO_2 mixed with mineral dust may be required to generate large-scale phytoplankton blooms (Meskhidze et al., 2005). Patagonia, the postulated source region for the dust used for the Fe fertilization of the Atlantic sector of the SO

(ASO), is sparsely populated and considered to be one of the most pristine areas of the globe. The amount of SO_2 available for mixing with mineral dust plumes is unlikely to be enough to acidify the dust and solubilize mineral-Fe; (iii) Due to highly dynamic nature of ACC, sampling frequencies significantly higher than the monthly averaged values, used in published mineral dust - phytoplankton growth study (Erickson et al., 2003), are required to reliably establish a correlation (Meredith et al., 2005); (iv) Mineral dust deposition fluxes and phytoplankton productivity downwind from Patagonia have similar seasonal trends: they both reach their maxima during September to March and diminish during austral fall and winter (Trenberth et al., 1990; Gaiero et al., 2003; Lässig et al., 1999). Therefore, removal of seasonal trends in the temporal anomalies is necessary.

Atmospheric circulation in Patagonia, an extended region of Argentina south of 42°S (Fig. 1), is controlled by strong and persistent westerlies (Labraga, 1994) and by the movement of dynamic cyclonic centers (Gaiero et al., 2003; Hoskins and Hodges, 2005). The low soil water content, sparse vegetation cover and strong surface winds yield significant dust emissions from Patagonia (Ginoux et al., 2001; Zender et al., 2003). Patagonian dust transport primarily occurs between 40°-60°S with the transport path that strongly correlates with the trajectories of cyclonic systems over the Atlantic and Indian Ocean regions of the SO (Hoskins and Hodges, 2005). The cyclogenesis and prevailing westerly winds that cause dust transport from Patagonia have also been shown to cause strong baroclinic instability in Atlantic and Indian Ocean regions of the SO (Taljaard, 1972; Trenberth, 1991; Nakamura and Shimpo, 2004; Hoskins and Hodges, 2005). Number of studies of the Southern Hemisphere “storm tracks” show that interaction of dynamic cyclones with baroclinically unstable frontal jets (see Supplementary

Information) may initiate meandering currents and lead to isolated up- and down-welling (Hense et al., 2003). Due to the high eastward velocities within the frontal zone, the meanders move eastward with typical wavelength of 160–180 km (Hense et al., 2003). The vertical velocities in mesoscale up-welling cells in ACC waters range from 5 to 20 m/day, leading to the comparable time scales for transporting cold and nutrient rich waters from below the mixed layer depth (40 to 120 m) and doubling the phytoplankton concentration in surface waters (Hense et al., 2003; Coale et al., 2004). As eddies contribute to cross frontal and vertical nutrient exchange, whey are often assumed to promote phytoplankton growth (e.g. Hense et al., 2003).

To explain the strong correlation between aeolian dust deposition and [Chl *a*] (Erickson et al., 2003), we suggest an existence of atmospheric circulation pattern in the region that simultaneously causes the uplift and transport of mineral dust from Patagonia and an upward supply of nutrient-rich waters from to the surface waters of ACC. (Unless otherwise noticed, “upwelling” or “upward supply” in this study is thought to primarily occur due to mesoscale circulation and frontal dynamics along ACC.) Such a mechanism, if it exists, would enhance ocean productivity in the ASO through upwelling but would still exhibit a high correlation between [Chl *a*] and atmospheric dust-Fe flux even if the dust did not contain significant amounts of bioavailable-Fe and thus played no actual role in fostering enhanced biological activity in the region. To check the viability of this mechanism we perform statistical analyses of remotely sensed sea surface temperature (SST) and [Chl *a*] data. Because relatively uniform near-surface temperatures in longitudinal direction (Peterson and Stramma, 1991) and high concentration of nutrients in the deep waters (Martin et al., 1990; de Baar et al., 1995; Löscher et al., 1997), SST anomalies can be used as a proxy for upwelling in ACC; i.e., negative SST anomalies would point to the regions where ocean productivity is likely to be supported by upward supply of relatively cold waters with enriched concentrations of nutrients (e.g., bioavailable-Fe). By examining the correlation of the weekly anomalies, we assess the response of [Chl *a*] departures to those of SST (see below). The correlation analyses is carried out in ASO between 20°S to 80°S and 80°W to 40°E (hereinafter referred to as study area) and the relative importance of oceanic and atmospheric sources of Fe are examined in the perspective of conditions needed for mobilization of mineral-Fe into bioavailable form (Meskhidze et al., 2005).

2. Materials and Methods

2.1 SST and [Chl *a*] correlation calculation

The 8-day averages of MODIS (Moderate Resolution Imaging Spectroradiometer) remotely sensed SST and [Chl *a*] data with 39 km special resolution (see Supplementary Information) are used to produce weekly anomaly maps. The weekly data was chosen to assure that the [Chl *a*] is not considerably affected by cloud variability, while still allowing the SST signal to retain the characteristics of its origin. Short averaging time also minimizes the wind drift of fertilized water masses. The SST and [Chl *a*] spatial anomalies were computed by subtracting the longitudinally averaged values (over 1° on either side) from the time series of data. The use of longitudinal averages was chosen because both [Chl *a*] and SST are relatively uniform along the ACC fronts. Data points characterizing clouds and continental regions were carefully removed from the analysis.

The regions of very low algal biomass are not relevant to the discussion; thus, the correlation coefficient calculations were limited to areas with yearly average [Chl *a*] > 0.2 mg m^{-3}. Lower values can also cause anomalous readings in retrievals of phytoplankton biomass (Claustre et al., 2002) and bias our analysis. Total suspended material (TSM) and colored dissolved organic matter (CDOM) in optically complex coastal waters near large river discharge and a relatively shallow sea floor regions (i.e., along the Patagonian coast) may also cause inaccurate retrieval of MODIS [Chl *a*] (Esaias, et al., 1998); therefore results of our analysis in near coastal regions should be regarded with some degree of caution.

3. Results and Discussion

3.1 [Chl *a*] concentration and the ocean circulation

Figure 2 shows seasonal and yearly-averaged [Chl *a*] images for the study area downwind from Patagonia. The figure indicates the appearance of a high [Chl *a*] region almost parallel to the Argentine coastline from ~35°S to 50°S as well as elongated west to east streaks downwind from Patagonia. The high [Chl *a*] region near the Argentine coast coincides with the location of the cold and nutrient rich Malvinas Current (see Fig. 2a); mesoscale meandering bands of elevated [Chl *a*] downwind from Patagonia seem to be well associated with the upper-level currents in ACC and trajectories of cyclonic systems (Hoskins and Hodges, 2005). Though [Chl *a*] in this regions is not as high as in Malvinas current, elevated marine productivity along the Subtropical Front is clearly visible over the negligible background [Chl *a*]. The source of the bioavailable-Fe causing the enhanced [Chl *a*] in remote waters of the SAO can not be definitively ascertained from Fig. 2 alone; however, the characteristic geometry and of the observed [Chl *a*] suggest that upwelling due to the interaction of cyclonic systems with rapidly flowing ACC currents is certainly plausible.

Figure 2 also shows that the waters surrounding South Georgia Island often support large phytoplankton blooms. The regularly observed stimulation of the primary production north of the Island is highly localized and correlates well with the peak frequency of seasonal dust advection off the Patagonian coast (see below). Although enhancement of productivity and biomass near South Georgia Island has been attributed to the ‘‘island-mass effect’’ leading to surface water becoming enriched in nutrients from the island platform (e.g., de Baar et al., 1995), the precise mechanism of bloom formation remains poorly understood (Korb and Whitehouse, 2004) and could be caused by episodic deposition of Patagonian dust. These suppositions are examined statistically below.

3.2. Remotely Sensed SST and [Chl *a*] anomaly correlation

If enhanced productivity in study area is driven by upwelling of cold and nutrient-rich (e.g., Fe) deep waters from below the euphotic zone, we would expect to find a negative correlation between SST and [Chl *a*] anomalies in the region. Comparison of Figs. 2 and 3 shows that the regions with elevated [Chl *a*] in the remote waters of the SAO also display negative correlation (-0.3 to -0.6) between the SST and [Chl *a*] anomaly fields, suggesting that biological activity in ACC is likely to be coupled to upwelling of Fe-rich waters. To get an objective measure of the strength of the correlation, we have chosen several zones in ACC region with elevated [Chl *a*] (see Fig. 2e), and calculated correlation coefficients for seasonally and yearly averaged SST and [Chl *a*] anomaly fields within these zones. Correlations for the seasonal anomalies were calculated to evaluate the response of [Chl *a*] to changes of SST for the seasonal cycle of the mixed layer depth, wind stress and solar irradiance levels, while yearly anomalies were calculated to assess the long term relationship between SST and [Chl *a*]. Fig. 4 shows that most of the zones display considerable negative correlation between SST and [Chl *a*]. The correlation is typically highest during the austral summer and fall likely caused by the shoaling of mixed layer depth (Hense et al., 2003) and increase in the zonal wind stress (Trenberth et al., 1990), making it easier for nutrients from below euphotic zone to be uplifted to the surface ocean. During austral summer and fall seasons, the SST and solar irradiance levels in ACC are also sufficient for sustaining high rates of photosynthesis (Moore and Abbott, 2002). The negative correlation between SST and [Chl *a*] shown on Figs. 3 and 4 supports the statement that the supply of dissolved Fe to the surface ocean of ACC is most likely from below by upwelling of cold and nutrient rich waters. However, Figs. 3 and 4 also show that in the large phytoplankton bloom area near South Georgia Island (zone 7) correlation is insignificant indicating that supply of bioavailable Fe by means other than upwelling of deep ocean waters (i.e., from atmospheric input of Patagonian dust) is plausible and will be discussed in details below.

Examining the time lag between remotely sensed SST and [Chl *a*] dataset provides further support for the deep water enrichment of Fe. It has been shown that primary productivity in an Fe-enriched patch of the ACC waters begins to exhibit a significant increase after several days of an initial infusion and [Chl *a*] levels remain noticeably enhanced for more than a month (Boyd et al., 2000; Abraham et al., 2000; Coale et al., 2004). If the enhanced [Chl *a*] is caused by the upwelled nutrients, as the rapid eastward flow in ACC moves the fertilized water masses away from the area of the enrichment, it is expected to see considerable de-correlation of SST and [Chl *a*] anomaly fields when time delay between two fields increases over several weeks. However, if [Chl *a*] increase is caused by deposition of mineral dust, assuming that dust is not preferentially deposited in the upwelling zones, there should be no significant change in the observed SST - [Chl *a*] correlation image with the time evolution. Figures 5a-b show that the correlation between two fields is typically high when the time delay between SST and [Chl *a*] is less than two weeks and diminishes as the delay increases further. More importantly, when the time series for [Chl *a*] are shifted behind of SST by more than one month, the correlation between the two fields virtually disappears (Fig. 5c).

Despite capturing some main features of phytoplankton distribution in study area, Figs. 3 and 4 show that negative correlation between SST and [Chl *a*] is not strong in all parts of ACC with elevated [Chl *a*]. The extensive cloud cover over the Southern Ocean is one of the factors that can significantly weaken the correlation between remotely sensed fields. Since sea surface temperature is collected at night as well as during the day SST coverage is generally better than ocean color data, which can only be collected during daylight hours. Although SST and [Chl *a*] data used in correlation analysis are from the same week, depending on cloud cover, parameters chosen for the weekly averages may be from different days. The correlation is farther hampered by geostrophic transport along the frontal jets (Strass et al., 2002); simulations of the regional ecosystem dynamics in the ACC show (in agreement with observations (Strass et al., 2002)) that in the meandering current, low phytoplankton concentrations can coincide with upwelling spots, whereas maximum [Chl *a*] concentrations can occasionally occur in downwelling areas (Hense et al., 2003). Eddies and cross-frontal circulation, sporadically produced by baroclinic instability along frontal currents can lead to redistribution of major nutrients and phytoplankton between surface and deep ocean. Newly-upwelled water near the surface has low [Chl *a*], but is rich in nutrients and therefore can sustain phytoplankton growth during its advection, until water is downwelled on the side of the meander ridge (Hense et al., 2003). If horizontal advection in ACC currents is fast enough to move the fertilized water masses outside of the MODIS observed grid domain, it can significantly lessen negative correlation between SST and [Chl *a*] and even reverse its sign. Other factors such as silicic acid, light limitations and the grazing pressure may also be significant at times. Therefore, highly complex behavior of ecosystem dynamics in ACC region can not be fully resolved by remotely sensed data; instead, in situ observations and comprehensive three-dimensional ocean-plankton models are required to fully account for the surface ocean - chlorophyll dynamics (Hense et al., 2003; Pollard et al., 2002).

The absence of correlation between SST and [Chl *a*] signals in the large phytoplankton bloom area close to South Georgia Island (zone 7 on Fig. 2a) can be explained by considering the possible mechanism for the bloom formation in these waters. Korb and Whitehouse (2004) suggest that anticyclonic circulation near South Georgia is capable of enriching the surface waters by sedimentary micronutrients (e.g., Fe) from the bottom waters and the island’s shelf. Reduced surface mixing and the retention of water near the surface caused by anticyclonic circulation can also result in stability and elevated temperatures initiating large phytoplankton blooms (Meredith et al., 2003; Korb and Whitehouse, 2004). Such mechanisms of bloom formation are not captured by the objective analysis used here and therefore, display no significant correlation between SST and [Chl *a*] anomalies in this region (Fig. 3).

3.3. Large bloom in the South Georgia region

As the precise mechanism for the bloom formation near South Georgia Island remains poorly understood (Korb and Whitehouse, 2004), we test the potential role of Patagonian dust deposition in the observed blooms. Fig. 6 illustrates MODIS observed [Chl *a*] concentrations downwind from the Island and MATCH (Model of Atmospheric Transport and Chemistry (Rasch et al., 1997; Mahowald et al., 1997) calculated fluxes of mineral dust (see also Figs. S2, S3). Although increase of biological activity in this region is a regular phenomenon with similar seasonal trend as Patagonian dust deposition (Fig. 6), there is significant variation in the bloom's temporal appearance, spatial extent and strength that can not be accounted by the variation in mineral dust. Large atmospheric dust fluxes in year 2000 did not cause significant change of [Chl *a*] in this region, while years 2001 and 2004 with moderate dust deposition were characterized by massive blooms. Although these results cannot be considered conclusive because MATCH results have not been tested extensively against surface observations in the Southern Hemisphere (Luo et al., 2003), they are suggestive that dust deposition is not a major controlling factor of enhanced productivity near South Georgia Island. Nevertheless, the detailed analyses of hydrographic data concurrently with in-situ studies of mineral dust composition and soluble Fe fraction may be necessary to unambiguously identify the sources of bioavailable Fe and their controls on biological productivity near South Georgia Island.

4. Possible Implications to Carbon Cycle in the ASO

Analysis of remotely-sensed MODIS data shows significant negative correlation (-0.3 to -0.6) between SST and [Chl *a*] spatial anomalies in study area of the SAO. Since SST anomalies in this region can be used as a proxy for upwelled nutrients (e.g., Fe), these correlations are likely to be indicative of a causal relationship between upwelling of nutrient-rich waters and ocean productivity in ASO. This result is consistent with our earlier studies supporting the hypothesis that substantial acidification of aeolian dust prior to it deposition to the ocean may be required to solubilize the large fraction of mineral-iron and make it bioavailable (Duce and Tindale, 1991; Zhuang et al., 1992; Zhu et al., 1993; Spokes and Jickells, 1996; Desboeufs et al., 2001; Meskhidze et al., 2003; 2005). In conjunction with previously shown high correlation between mineral dust-Fe deposition and [Chl *a*] (Erickson et al., 2003), results of this study suggest the existence of a meteorological mechanism that simultaneously uplifts and transports mineral dust from Patagonia and drives deep-water upwelling of nutrients (e.g., dissolved-Fe) to the surface waters of the ASO.

To the extent that biological activity in this region plays an important role in global carbon cycle, the results presented in this study in conjunction with our previous analysis of mineral dust transport (Meskhidze et al., 2005) suggest that mere changes in the dust-Fe supply (perhaps without significant increase in sulfur sources) may not exert considerable influence on the drawdown of atmospheric CO_2 in the ASO. So, if past changes in the supply of bioavailable Fe to the ASO have played nontrivial role in determining the atmospheric CO_2, the hypothesis about the required acidity for mobilizing significant fraction of DIF in dust may prove to be invaluable in understanding the dynamics of the past climate.

Acknowledgements. This work was supported by NSF CAREER grant, a Blanchard-Milliken Junior Faculty Fellowship and from Georgia Tech Faculty Startup funds. We thank Yoram Kaufman and Emanuele Di Lorenzo for constructive discussions and two anonymous reviewers for their thoughtful comments.

References

Abraham, E.R., C.S. Law, P.W. Boyd, S.J. Lavender, M.T. Maldonado, and A.R. Bowie (2000), Importance of stirring in the development of an iron-fertilized phytoplankton bloom, *Nature, 407*, 727-730.

Banse, K. (1996) Low seasonality of low concentrations of surface chlorophyll in the Subantarctic water ring: underwater irradiance, iron, or grazing? *Prog. Oceanogr. 37*, 241–291.

Bay, R.C., N. Bramall, and P.B. Price (2004), Bipolar correlation of volcanism with millennial climate change *Proc. Natl. Acad. Sci. USA, 101*, 6341-6345.

Bonnet, S., and C. Guieu (2004), Dissolution of atmospheric iron in seawater, *Geophys. Res. Lett.*, *31*, L03303, doi:10.1029/2003GL018423.

Boyd, P. W., G. McTainsh, V. Sherlock, K. Richardson, S. Nichol, M. Ellwood, and R. Frew (2004), Episodic enhancement of phytoplankton stocks in New Zealand subantarctic waters: Contribution of atmospheric and oceanic iron supply, *Global Biogeochem. Cycles*, *18*, GB1029, doi:10.1029/2002GB002020.

Boyd, P.W. Watson, A.J., Law, C.S., Abraham, E.R., Trull, T., Murdoch, R., Bakker, D.C.E., Bowie, A.R., Buesseler, K.O., Chang, H., et al. (2000), A mesoscale phytoplankton bloom in the polar Southern Ocean stimulated by iron fertilization, *Nature, 407*, 695-702.

Boyd, P.W., A.C. Crossley, G.R. DiTullio, F.B. Griffiths, D.A. Hutchins, B. Queguiner, P.N. Sedwick, T.W. Trull (2001), Control of phytoplankton growth by iron supply and irradiance in the subantarctic Southern Ocean: experimental results from the SAZ project. *J. Geophys. Res. 106*, 31,573– 31,583.

Bradshaw, J., D. Davis, G. Grodzinsky, R. Newell, S. Sandholm, S. Liu and S. Smyth (2000), Observed distributions of nitrogen oxides in the remote free troposphere from the NASA global tropospheric experiment programs, *Rev. Geophys. 38*, 61-116.

Brandini, F.P., D. Boltovskoy, A. Piola, S. Kocmur, R. Röttgers, P.C. Abreu, and R.M. Lopes (2000), Multiannual trends in fronts and distribution of nutrients and chlorophyll in the southwestern Atlantic (30-62 degrees S), *Deep-Sea Res. I, 47*, 1015-1033.

Charlson, R.J., J.E. Lovelock, M.O. Andreae, and S.G. Warren (1987), Oceanic phytoplankton, atmospheric sulfur, cloud albedo and climate, *Nature, 326*, 655-661.

Chin, M., R.B. Rood, S.J. Lin, J.F. Muller, and A.M. Thompson (2000), Atmospheric sulfur cycle simulated in the global model GOCART: Model description and global properties, *J. Geophys. Res.*, *105,* 24,671-24,687.

Claquin, T., M. Schulz, and Y.J. Balkanski (1999), Modeling the mineralogy of atmospheric dust sources *J. Geophys. Res*. *104*, 22,243-22, 256.

Claustre, H. A. Morel, S.B. Hooker, M. Babin, D. Antoine, K. Oubelkheir, A. Bricaud, K. Leblanc, B. Queguiner, and S. Maritorena (2002), Is desert dust making oligotrophic waters greener?, *Geophys. Res. Lett.*, *29*, 1469, 10.1029/2001GL014056.

Coale, K.H., K.S. Johnson, F.P. Chavez, K.O. Buesseler, R.T. Barber, M.A. Brzezinski, et al., (2004), Southern ocean iron enrichment experiment: Carbon cycling in high- and low-Si waters, *Science, 304*, 408-414.

Coale, K.H., K.S. Johnson, S.E. Fitzwater, R.M. Gordon, S. Tanner, F.P. Chavez, L. Ferioli, C. Sakamoto, P. Rogers, F. Millero, P. Steinberg, P. Nightingale, D. Cooper, W.P. Cochlan, M.R. Landry, J. Constantinou, G. Rollwagen, A. Trasvina, and R. Kudela (1996), A massive phytoplankton bloom induced by an ecosystem-scale iron fertilization experiment in the equatorial Pacific Ocean, *Nature*, *383*, 495-501.

Colin, J.L., J.L. Jaffrezo, and J.M. Gros (1990), Solubility of major species in precipitation - factors of variation, *Atmos. Environ. 24,* 537-544.

de Baar, H. J. W. and P. W. Boyd, Distributions, sources and sinks of iron in seawater, in *The Dynamic Ocean Carbon Cycle: A Midterm Synthesis of the Joint Global Ocean Flux Study*, (eds. Hanson, R. B., Ducklow, H. W. & Field, J. G.) 61– 140 (Cambridge Univ. Press, New York, 2000)

de Baar, H.J.W., J.T.M. de Jong , D.C.E. Bakker, B.M. Loscher, C. Veth, U. Bathmann, and V. Smetacek (1995), Importance of iron for plankton blooms and carbon-dioxide drawdown in the southern-ocean, *Nature*, *373,* 412-415.

Dentener, F.J. and P.J. Crutzen (1994), A 3-dimensional model of the global ammonia cycle, *J. Atmos. Chem.*, *19*, 331-369.

Desboeufs, K. V., R. Losno, and J. L. Colin (2001), Factors influencing aerosol solubility during cloud processes, *Atmos. Environ*., *35*, 3529–3537.

Duce, R.A. and N.W. Tindale (1991), Atmospheric transport of iron and its deposition in the ocean, *Limnol. Oceanogr*., *36*, 1715-1726.

Dugdale, R. C., and F. P. Wilkerson (1998), Silicate regulation of new production in the equatorial Pacific upwelling, Nature, 391, 270–273.

Esaias, W. E., M. R. Abbott, I. Barton, O. B. Brown, J. W. Campbell, K. L. Carder, D. K. Clark, R. H. Evans, F. E. Hoge, H. R. Gordon, W. M. Balch, R. Letelier, and P. J. Minnett, (1998) An overview of MODIS capabilities for ocean science observations, *IEEE Trans. Geosci. Remote Sensing*, 36, 1250- 1265.

Erickson, D.J., J.L. Hernandez, P. Ginoux, W.W. Gregg, C. McClain, and J. Christian (2003), Atmospheric iron delivery and surface ocean biological activity in the Southern Ocean and Patagonian region, *J. Geophys. Res. Lett.*, *30*, doi:10.1029/2003GL017241.

Fung, I.Y., Meyn, S.K., Tegen, I., Doney, S.C., John, J.G., and Bishop, J.K.B. (2000), Iron supply and demand in the upper ocean, *Global Biogeochem. Cycles*., *14*, 281-295.

Gabric, A.J., R. Cropp, G.P. Ayers, G. McTainsh, and R. Braddock (2002), Coupling between cycles of phytoplankton biomass and aerosol optical depth as derived from SeaWiFS time series in the Subantarctic Southern Ocean, *Geophys. Res. Lett., 29*, doi:10.1029/2001GL013545.

Gaiero, D.M., J.L. Probst, P.J. Depetris, S.M. Bidart, and L. Leleyter (2003), Iron and other transition metals in Patagonian riverborne and windborne materials: Geochemical control and transport to the southern South Atlantic Ocean, *Geochim. Cosmochim. Acta, 67*, 3603-3623.

Ginoux, P., M. Chin, I. Tegen, J.M. Prospero, B. Holben, O. Dubovik, and S-J. Lin (2001) Sources and distributions of dust aerosols simulated with the GOCART model, *J. Geophys. Res.*, *106*, 20,255-20,273.

Hense, I., R. Timmermann, A. Beckmann, and U.V. Bathmann (2003), Regional ecosystem dynamics in the ACC: simulations with a three-dimensional ocean-plankton model, *Journal of Marine Systems, 42***,** 31– 51.

Hoskins B.J. and K.I. Hodges (2005), A new perspective on Southern Hemisphere storm tracks, *Journal of Climate*, *18*, 4108-4129.

Jickells, T.D. and L.J. Spokes, Atmospheric iron inputs to the oceans, in *The biogeochemistry of iron in seawater*, edited by D.R. Turner, and K.A. Hunter, pp. 85-121, J. Wiley & Sons, New York, 2001.

Korb, R.E. and M. Whitehouse (2004), SeaWiFS in the southern ocean: spatial and temporal variability in phytoplankton biomass around South Georgia, *Deep-Sea Research I*, *51*, 721–738

Labraga, J.C. (1994**)**, Extreme winds in the pampa-del-castillo plateau, patagonia, argentina, with reference to wind farm settlement, *J. Appl. Meteorol., 33*, 85-95**.**

Lässig, J.L., M.G. Cogliati, M.A. Bastanski, and C. Palese (1999), Wind characteristics in Neuquen, North Patagonia, Argentina, *J. Wind Eng. Ind. Aerodyn*., *79*, 183-199.

Latimer, J.C. and G.M. Filippelli (2001), Terrigenous input and paleoproductivity in the Southern Ocean, *Paleoceanography*, *16*, 627–643.

Lefèvre, N. and A.J. Watson (1999), Modeling the geochemical cycle of iron in the oceans and its impact on atmospheric CO_2 concentrations *Global Biogeochem. Cycles*, *13*, 727-737.

Löscher, B.M., H.J.W. de Baar, J.T.M. de Jong, C. Veth, and F. Dehairs (1997), The distribution of Fe in the Antarctic Circumpolar Current *Deep-Sea Res. II 44*, 143-187.

Luo, C., N.M. Mahowald, and J. del Corral (2003), Sensitivity study of meteorological parameters on mineral aerosol mobilization, transport, and distribution, *J. Geophys. Res.*, *108***,** doi:10.1029/2003JD003483.

Maher, B.A., and P.F. Dennis (2001) Evidence against dust-mediated control of glacial-interglacial changes in atmospheric CO_2, *Nature* 411, 176-180.

Mahowald, N. M., P. J. Rasch, B. E. Eaton, S. Whittleston, and R. G. Prinn (1997), Transport of 222 radon to the remote troposphere using MATCH and assimilated winds from ECMWF and NCEP/NCAR, *J. Geophys. Res.*, *102*, 28,139–28,151.

Martin, J.H. and S.E. Fitzwater (1988), Iron-deficiency limits phytoplankton growth in the northeast pacific subarctic, *Nature*, *331*, 341-343.

Martin, J.H., R.M. Gordon, and S.E. Fitzwater (1990), Iron in Antarctic waters, *Nature, 345*, 156-158.

Meredith, M.P., J.L. Watkins, E.J. Murphy, N.J. Cunningham, A.G. Wood, R. Korb, M.J. Whitehouse, SE. Thorpe, and F. Vivier (2003), An anticyclonic circulation above the Northwest Georgia Rise, Southern Ocean, *Geophys. Res. Lett*., *30*, 2061, doi:10.1029/2003GL018039.

Meredith, M. P., and C. W. Hughes (2005), On the sampling timescale required to reliably monitor interannual variability in the Antarctic circumpolar transport, *Geophys. Res. Lett.*, *32*, L03609, doi:10.1029/2004GL022086.

Meskhidze, N., W.L. Chameides, A. Nenes, and G. Chen (2003), Iron mobilization in mineral dust: Can anthropogenic SO2 emissions affect ocean productivity?, *Geophys. Res. Lett.*, *30*, doi:10.1029/2003GL018035.

Meskhidze, N., W.L. Chameides, and A. Nenes (2005), Dust and pollution: A recipe for enhanced ocean fertilization? *J. Geophys. Res*. *110*, D03301, doi:10.1029/ 2004JD005082.

Mitchell, B.G., E.A. Brody, O. Holm-Hansen, C. McClain, J. Bishop (1991), Light limitation of phytoplankton biomass and macronutrient utilization in the Southern Ocean. *Limnol. Oceanogr., 36*, 1662– 1677.

Moore, J. K. and M. R. Abbott (2002), Surface chlorophyll concentrations in relation to the Antarctic Polar Front: seasonal and spatial patterns from satellite observations, *J. Marine Syst.*, *37*, 69-86.

Nakamura, H., and A. Shimpo (2004) Seasonal variations in the Southern Hemisphere storm tracks and jet streams in a reanalysis dataset. *J. Climate*, 17, 1828–1844.

Peterson, R.G., and L. Stramma (1991), Upper-level circulation in the South-Atlantic Ocean, *Prog. Oceanogr*., *26*, 1-73.

Pollard, R.T., M.I. Lucas, and J.F. Read (2002), Physical controls on biogeochemical zonation in the Southern Ocean *Deep-Sea Res. II, 49,* 3289–3305.

Rasch, P.J., N.M. Mahowald, and B. E. Eaton (1997), Representations of transport, convection, and the hydrologic cycle in chemical transport models: Implications for the modeling of short-lived and soluble species, *J. Geophys. Res*., *102*, 18127-18138.

Röthlisberger, R., Bigler, M., Wolff, E.W., Joos, F., Monnin, E., and Hutterli, M.A. (2004), Ice core evidence for the extent of past atmospheric CO_2 change due to iron fertilization, *Geophys. Res. Lett*., *31*, doi:10.1029/2004GL020338.

Smetacek, V., H.J.W. de Baar, U.V. Bathmann, K. Lochte, and M.M.R. Van der Loeff (1997), Ecology and biogeochemistry of the Antarctic Circumpolar Current during austral spring: a summary of Southern Ocean JGOFS cruise ANT X/6 of R.V. Polavstern, *Deep-Sea Res. II* , *44*, 1-21.

Spokes, L., and T. D. Jickells (1996), Factors controlling the solubility of aerosol trace metals in the atmosphere and on mixing into seawater, Aquat. Chem., 1, 355– 374.

Strass, V.H., A.C.N. Garabato, R.T. Pollard, H.I. Fischer, I. Hense, J.T. Allen, J.F. Read, H. Leach, and V. Smetacek (2002), Mesoscale frontal dynamics: shaping the environment of primary production in the Antarctic Circumpolar Current, *Deep-Sea Research II*, *49*, 3735 – 3769.

Taljaard, J.J., (1972), Synoptic meteorology of the Southern Hemisphere. In *Meteorology of the Southern Hemisphere*, Newton C.W. (ed.). Meteorol. Monogr.13, American Meteorological Society, Boston, MA; 139–213.

Trenberth, K.E., W.G. Large, and J.G. Olson (1990), The mean annual cycle in global ocean wind stress *J. Phys. Oceanogr.*, *20*, 1742-1760.

Trenberth, K. E., (1991), Storm tracks in the Southern Hemisphere. *J. Atmos. Sci.*, 48, 2159–2178.

Watson, A.J., Iron limitation in the oceans, in *The biogeochemistry of iron in seawater*, (eds. Turner, D.R. & Hunter, K.A.) 85-121 (Wiley & Sons, New York, 2001).

Watson, A.J., D.C.E. Bakker, A.J. Ridgwell, P.W. Boyd, and C.S. Law (2000), Effect of iron supply on Southern Ocean CO_2 uptake and implications for glacial atmospheric CO_2, *Nature, 407*, 730-733.

Zender, C.S., H.S. Bian, and D Newman (2003), Mineral Dust Entrainment and Deposition (DEAD) model: Description and 1990s dust climatology, *J. Geophys. Res., 108*, 4416. doi:10.1029/2002JD002775.

Zhu, X., J.M. Prospero, D.L. Savoie, F.J. Millero, R.G. Zika, and E.S. Saltzman (1993), Photoreduction of iron (III) in marine mineral aerosol solutions, *J. Geophys. Res. 98*, 9039-9046.

Zhuang, G., Z. Yi, R.A. Duce, and P.R. Brown (1992), Link between iron and sulphur cycles suggested by detection of Fe(II) in remote marine aerosols, *Nature, 355*, 537-539.

Figure Captions

Figure 1 Map of the South Atlantic Ocean (SAO).

Figure 2. MODIS-observed [Chl *a*] over the Atlantic sector of the Southern Ocean (ASO), averaged for the period from (a) September to November 2002, (b) December 2002 to February 2003, (c) March to May 2003, (d) June to August 2003, (e) September 2002 to August 2003. The thin white lines indicate the coastal boundary. Thick white lines on Fig. 1a denote the large-scale, upper-level currents and fronts in the ASO (adopted from Peterson and Stramma, 1991). White squares on Fig. 1e show the zones where seasonal variation of SST and [Chl *a*] anomaly correlation was calculated.

Figure 3. MODIS-observed yearly averaged (September 2002 to August 2003) SST and [Chl *a*] anomaly correlation for the ASO. The white lines indicate the coastal boundary. Gray color shows the area that was not included in correlation coefficient analysis ([Chl *a*] <0.2 mg m^{-3}).

Figure 4. Correlation coefficient for seasonally and yearly averaged MODIS-observed SST and [Chl *a*] anomaly correlation for the selected zones (see Fig. 1e) in ASO.

Figure 5. Same as for Figure 3, but with time series of [Chl *a*] shifted behind of SST by (a) 8-days, (b) 16-days and (c) 32-days.

Figure 6. (a) Latitudinally averaged (49°S to 54°S) MODIS-observed [Chl *a*] and (b) model predicted monthly averaged fluxes of mineral dust near South Georgia Island (49°-54°S, 35°–41°W). Horizontal dashed lines indicate the approximate area near the Island where the dust fluxes are averaged.

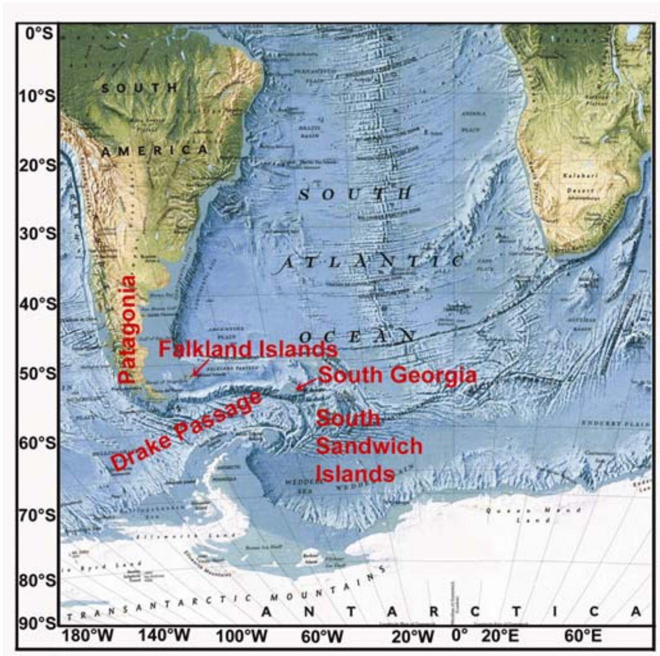
0°S
10°S
20°S
30°S
40°S
50°S
60°S
70°S
80°S
90°S
180°W
140°W
100°W
60°W
20°W
0°
20°E
60°E
SOUTH
AMERICA
SOUTH
ATLANTIC
OCEAN
Patagonia
Falkland Islands
South Georgia
Drake Passage
South
Sandwich
Islands
TRANSANTARCTIC MOUNTAINS
ANTARCTICA

Figure 1

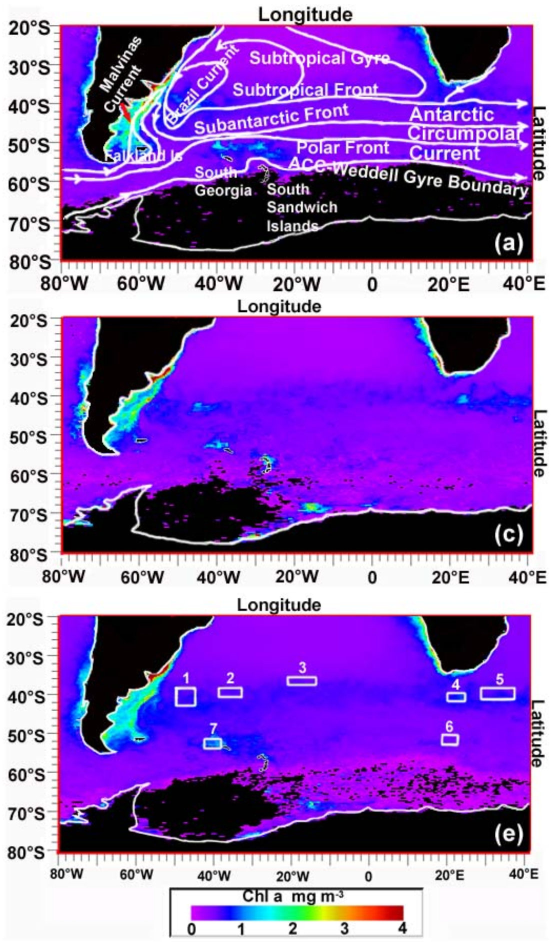

Longitude
Latitude
Malvinas Current
Brazil Current
Subtropical Gyre
Subtropical Front
Subantarctic Front
Antarctic Circumpolar Current
Polar Front
Falkland Is
ACC-Weddell Gyre Boundary
South Georgia
South Sandwich Islands
(a)
(b)
(c)
(d)
(e)
20°S
30°S
40°S
50°S
60°S
70°S
80°S
80°W
60°W
40°W
20°W
0
20°E
40°E
1
2
3
4
5
6
7
Chl a mg m-3
0
1
2
3
4

Figure 2

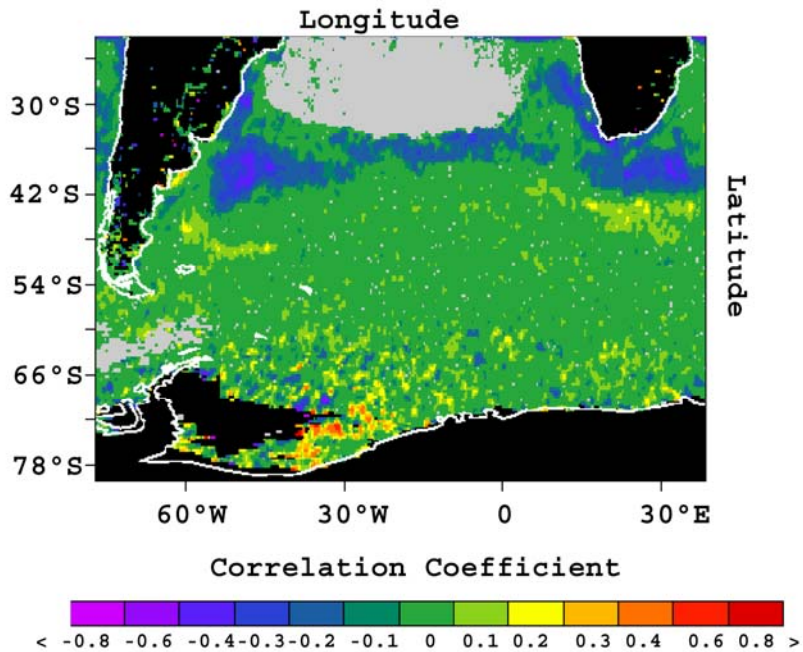
Longitude
30°S
42°S
54°S
66°S
78°S
60°W
30°W
0
30°E
Latitude
Correlation Coefficient
< -0.8 -0.6 -0.4 -0.3 -0.2 -0.1 0 0.1 0.2 0.3 0.4 0.6 0.8 >

Figure 3

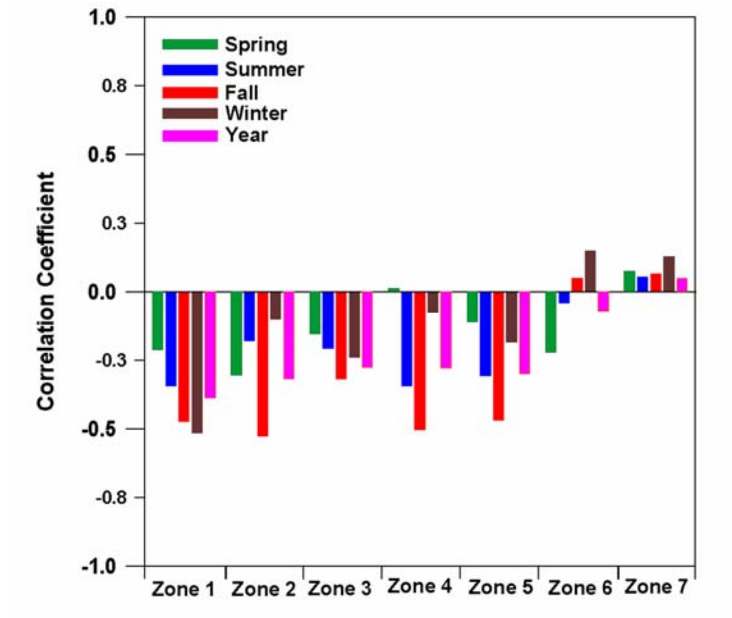

Spring
Summer
Fall
Winter
Year
Correlation Coefficient
1.0
0.8
0.5
0.3
0.0
-0.3
-0.5
-0.8
-1.0
Zone 1
Zone 2
Zone 3
Zone 4
Zone 5
Zone 6
Zone 7

Figure 4

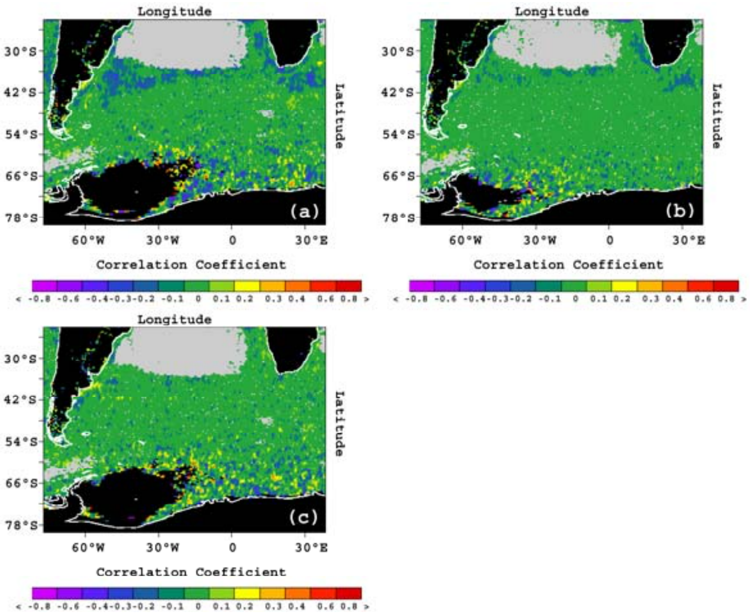
Longitude
30°S
42°S
54°S
66°S
78°S
Latitude
(a)
(b)
(c)
60°W
30°W
0
30°E
Correlation Coefficient
< -0.8 -0.6 -0.4 -0.3 -0.2 -0.1 0 0.1 0.2 0.3 0.4 0.6 0.8 >

Figure 5

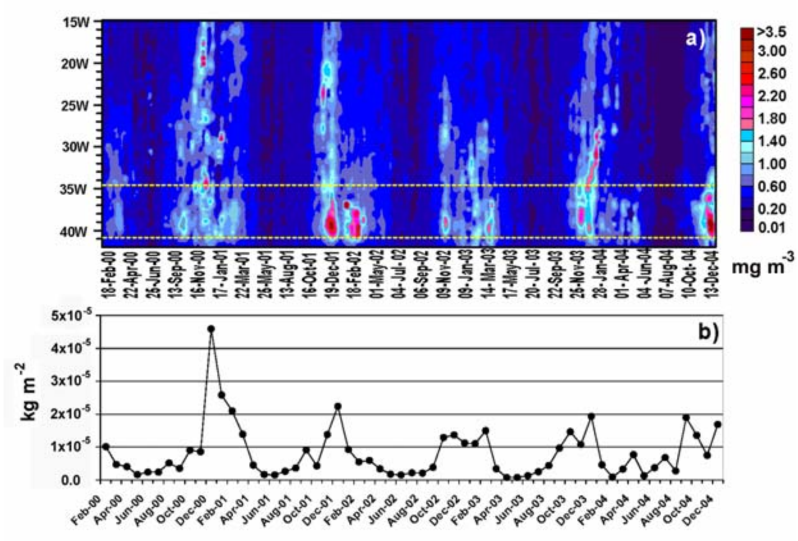

Figure 6

Supporting Online Material

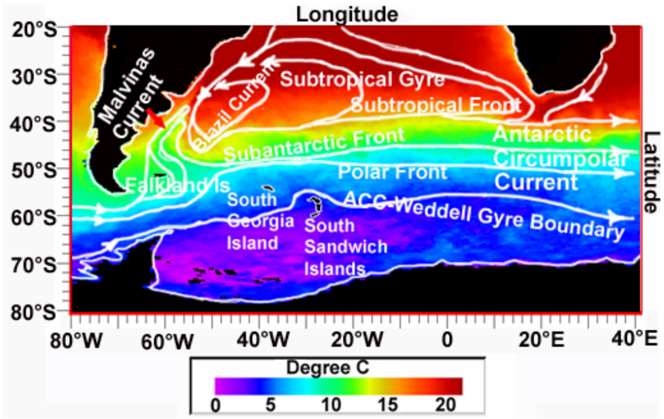

Figure S1. MODIS-observed SST over the subantarctic SAO averaged for the period from September 2002 to August 2003. Thick white lines denote the large-scale, upper-level currents and fronts in the South Atlantic Ocean (adopted from Peterson and Stramma, 1991). The thin white lines indicate the coastal boundary.

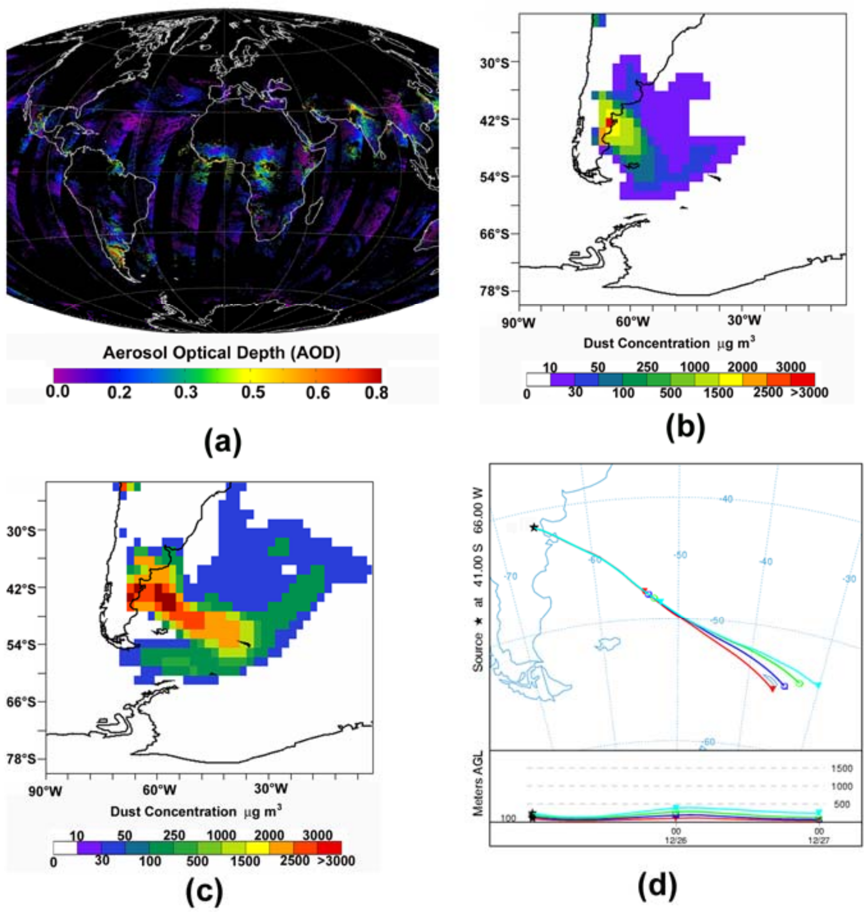

Figure S2. (a) MODIS observed aerosol optical depth (AOD) for December 25, 2000, MATCH predicted surface concentration of dust for (b) December 25, 2000, (c) December 26, 2000, and (d) HYSPLIT predicted trajectories for December 25, 2000. Dust plume altitude is given in meters above ground level (AGL). Star indicates the assumed location for the origin of the plume, and the triangles are used to denote 24-hour intervals.

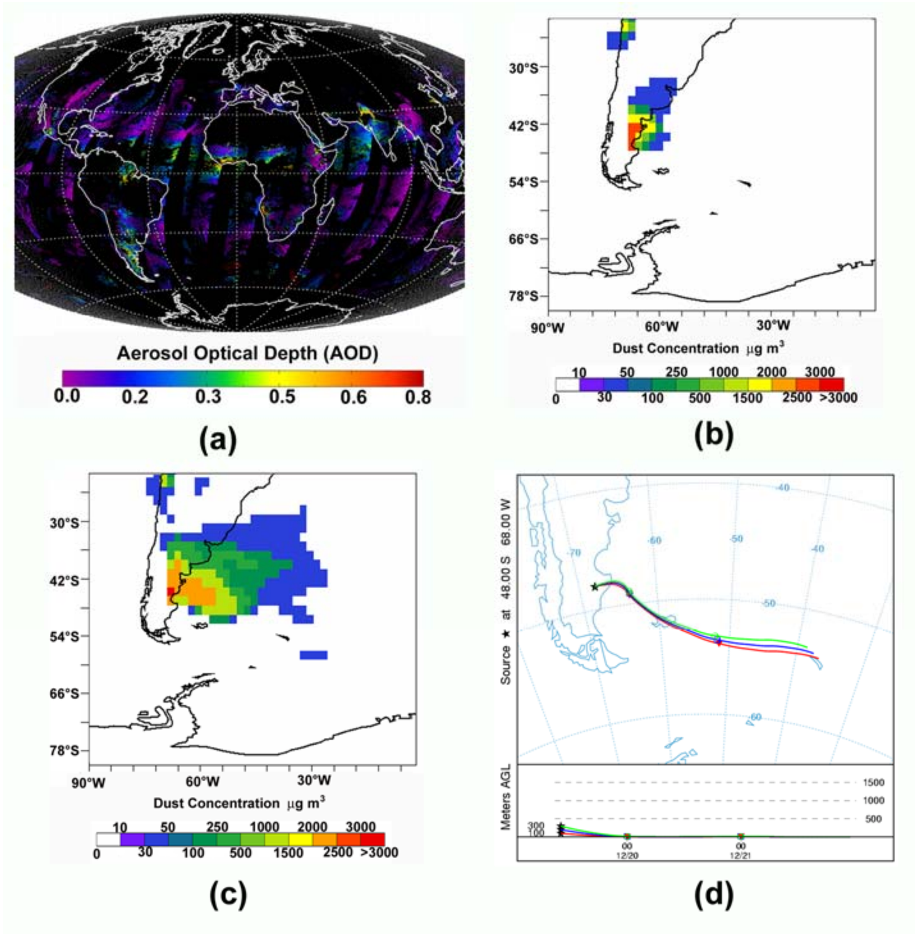

Figure S3. (a) MODIS observed aerosol optical depth (AOD) for December19, 2001, MATCH predicted surface concentration of dust for (b) December 19, 2001, (c) December 20, 2001, and (d) HYSPLIT predicted trajectories for December 19, 2001. Dust plume altitude is given in meters above ground level (AGL). Star indicates the assumed location for the origin of the plume, and the triangles are used to denote 24-hour intervals.

Supplementary Information

Ocean circulation

The eastward flow of ACC is not uniform, but dynamically constrained into narrow bands of fast flowing currents (fronts) that are identified in Fig. S1) as, from north to south, the Subtropical Front, the Subantarctic Front, the Polar Front and the ACC-Weddell Gyre Boundary (Peterson and Stramma, 1991). Because of high stratification of the ACC fronts, the banding is based on the observations of sharp stepwise changes in surface temperature and salinity (Peterson and Stramma, 1991). Additional South Atlantic currents relevant for our analysis are the Malvinas (Falkland) and Brazilian Currents (Fig. S1). Temperature-salinity relations and horizontal distribution of density and nutrients suggest that the Malvinas Current is a branch of the ACC that, after passing through the Drake Passage (Fig. 1), flows northward along the continental shelf of Argentina until it reaches the oligotrophic waters of the Brazil Current at about 40°S. At this point, the current retroflects back toward the south creating the Brazil-Malvinas Confluence Zone (Peterson and Stramma, 1991). Observations of sharp gradients in temperature, salinity and nutrients are often used to identify the boundary between the northward-flowing strong, relatively fresh, cold and nutrient-rich Malvinas Current and the southward-flowing weak, warm, and nutrient-poor Brazil Current (Brandini et al., 2000).

MODIS Data

Data collected by Moderate Resolution Imaging Spectroradiometer (MODIS) located on board of the EOS Terra satellite was used to monitor changes in Sea Surface

Temperature (SST) and Chlorophyll *a* concentration, [Chl *a*]. MODIS is an optical scanner that provides images of the Earth's land, ocean and atmosphere in 36 spectral bands (from 0.4μm to 14.5μm) with spatial resolution ranging from 250 meters to 1 kilometer. Data are processed by both the Goddard Distributed Active Archive Center (Goddard DAAC) and the MODIS Adaptive Processing System (MODAPS). Processing occurs in stages, producing different levels of data. Ocean color and SST are available at processing level 2 and 3 with a variety of time- and space-binned averages (on the web: //daac.gsfc.nasa.gov/data/).

Because MODIS is not able to monitor ocean surface conditions through clouds, there is a significant amount of patchiness in the data for any given satellite pass over the subantarctic South Atlantic Ocean. More complete spatial coverage can be obtained by compiling the results from multiple passes of the satellite over the same region. In this work we make use of weekly mean values of MODIS SST and ocean color data products (MO04MW), with each weekly mean being composite of data from 8 satellite passes. Each weekly-averaged composite used is a level 3 mapped product with 39 km special resolution and is contained in the associated HDF-EOS files. Detailed documentation on MO04MW data products can be fond on the web at: //daac.gsfc.nasa.gov/MODIS/ Terra/ocean/MO04MW.shtml.

WebWinds

Satellite images shown here were prepared using WebWinds interactive science data visualization system applied to the aforementioned MODIS level 3 weekly-averaged products. This WebWinds software is written in Java and available for all major computer platforms. Software is able to read and geo-reference MODIS level 1-3 data and display it as a false color image over a digital elevation map on a globe or plane. WebWinds is distributed by Open Channel Foundation (on the web: www. openchannelsoftware.com/projects/WebWinds/).